Underwater Visible Light Mobile Communication Using a Gain Feedback Control Method With Dynamic Threshold

Jiehui Liu, Lin Ma, *Senior Member, IEEE*, and Zuyuan He, *Senior Member, IEEE*

***Abstract*—In underwater visible light communication (UVLC) systems, it is important to support mobility of transceivers and enhance both the dynamic range of communication distance and the field of view (FOV) because the received optical power experiences significant variations when the transmission distance changes due to substantial intrinsic absorption of water. In this paper, we propose an UVLC system with mobility of transceivers using a gain feedback control (GFC) method with dynamic threshold, which obtains significant improvements in both the dynamic range of communication distance and FOV. In experiments, we achieved duplex mobile video transmission at a data rate of 5.0 Mb/s while moving at a speed of 0.21 m/s. Real-time duplex video transmission with a resolution of 800 × 600 pixels was realized at a distance ranging from 1.3 m to 5.6 m. The dynamic range of communication distance can be increased by a factor of 10.0 and 10.5 in comparison with the system without GFC at forward bias currents of 0.3 A and 0.35 A, respectively. In addition, the receiving FOV angle of the system is increased by a factor of 1.9.**

***Index Terms*—Underwater visible light communication (UVLC), duplex video transmission, gain feedback control (GFC).**

I. Introduction

RECENTLY, underwater visible light communication (UVLC) technologies have attracted a lot of attention due to their superior transmission speed and information security compared to traditional underwater acoustic and wireless communication systems. Many studies have been conducted with the aim of increasing both communication data rate and distance. A two-dimensional bit allocation nonlinear hybrid modulation underwater simplex system, achieving a data rate of 3.24 Gb/s over a distance of 1.2 m, has been reported [1], [2], [3]. Simplex communication with a data rate of 15.73 Gb/s over a distance of 1.6 m was achieved by combining four-wavelength multiplexing in the visible light region and a forward error correction coding technique [4]. Duplex 20 Mb/s transmission over a distance of 120 m were demonstrated in a deep-sea field trial [5]. In addition, the commercial optical communication system BlueComm 200 has successfully achieved UVLC with a data rate of 10 Mb/s up to a distance of 150 m [6]. However, modulation and equalization achieve higher data rate and spectral efficiency, which result in more severe optical power loss [7], [8]. The received optical power changes significantly as a function of communication distance due to substantial intrinsic absorption of water, and is also influenced by the system's FOV and is susceptible to obstacles, turbulence, and variations in water transparency [9], [10], [11], [12]. Consequently, signals in higher data rate typically result in shorter communication distances. In practical communication applications, it is important to support mobility of transceivers and increase both the dynamic range of communication distance and the FOV of the receiver for UVLC systems. Some research on visible light communication (VLC) supporting user-mobility in indoor, cell ID-based, and industrial environments has been carried out [13], [14], [15]. Different from the indoor scenario, more severe fluctuations in VLC channel gain caused by the mobility of transceivers in underwater application, this may result in detrimental outages in the instantaneous signal to noise ratio (SNR). Some studies are dedicated to exploring ways to enhance the dynamic range of receivers. Authors proposed an adaptive control strategy based on a photomultiplier tube (PMT) receiver to extend the dynamic range of received optical power to 68 dB over a distance of 2 m [16]. However, mobile experiments for underwater transceivers have not yet been conducted. The authors successfully demonstrated a 450-nm-laser/scintillating-fiber-based mobile UVLC over a 1 m working range to extend system's FOV [17]. However, the scintillating-fiber introduces significant self-interference in the system. Additionally, dynamic threshold schemes are employed to enhance the performance of VLC systems with mobility of transceivers. An adaptive feedback threshold (AFT) algorithm, relying on a one-time training sequence and feedback data statistics, has been proposed to achieve 120 Kb/s mobile transmission at a speed of 1 m/s in a visible light communication and positioning (VLCP) system [18]. However, the dynamic range of system is limited when it relies only on dynamic threshold to accommodate fluctuations in received signal intensity.

In this paper, we demonstrate an UVLC system with mobility of transceivers using a GFC method with dynamic threshold, which obtains significant improvements in both the dynamic range of communication distance and FOV. In experiments, we

Manuscript received 5 September 2023; revised 27 October 2023; accepted 13 November 2023. Date of publication 15 November 2023; date of current version 27 November 2023. The work was supported in part by the National Natural Science Foundation of China under Grant 62275150, and in part by Henan Key Laboratory of Visible Light Communications under Grant HKLVLC2023-B07. *(Corresponding author: Lin Ma.)*

The authors are with the State Key Laboratory of Advanced Optical Communication Systems and Networks, Shanghai Jiao Tong University, Shanghai 200240, China (e-mail: ma.lin@sjtu.edu.cn).

Digital Object Identifier 10.1109/JPHOT.2023.3333227

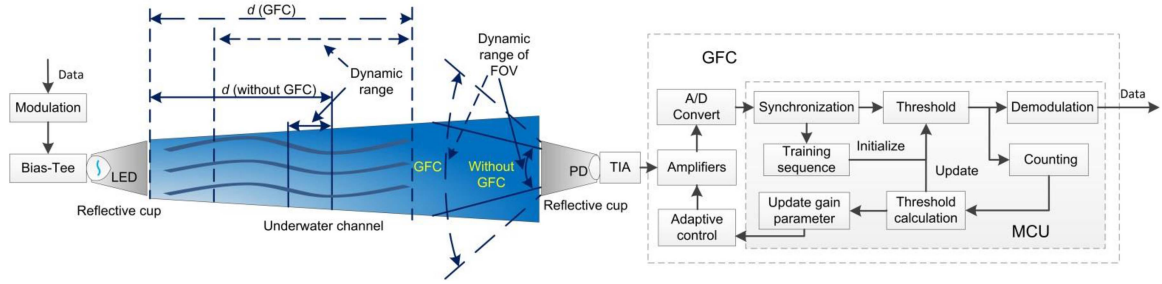

Fig. 1. Underwater visible light communication with a GFC method with dynamic threshold.

achieved duplex mobile video transmission with a data rate of 5.0 Mb/s at a moving speed of 0.21 m/s. Real-time duplex video transmission with a resolution of 800 × 600 pixels was realized at a distance ranging from 1.3 m to 5.6 m. Under a bit error rate (BER) threshold of 3.8×10^{-3}, the dynamic range of communication distance is increased by a factor of 10.0 and 10.5 in comparison with the system without GFC at forward bias currents of 0.3 A and 0.35 A, respectively. In addition, the receiving FOV angle of the system is increased by a factor of 1.9. To the best of our knowledge, this is the first paper reporting on real-time duplex underwater visible light mobile communication. A low-cost, high-integrated system and GFC method with dynamic threshold can effectively improve the stability and reliability of UVLC system with mobility of transceivers, which may have good potential in underwater mobile communication applications.

II. Theoretical Calculation and Simulation

A. System Model

As depicted in Fig. 1, the proposed system utilizes a LED as the light source and a positive-intrinsic-negative (PIN) detector as the receiver, respectively. There is a relationship between the received illuminance L of the PIN detector and the photocurrent I_{ss}, that is

$$L = I_{ss}n + m, \tag{1}$$

where m and n are constants. The received signal V_{out} is

$$V_{out} = \left(\frac{\psi}{Sn} - \frac{m}{n}\right) g_m G_g, \tag{2}$$

where S is the effective detection area of the receiver, ψ is the luminous flux illuminated over S, g_m is the trans-impedance of the trans-impedance amplifier (TIA), G_g is the gain control parameter.

In our study, Monte Carlo simulation were used to fit the double exponential attenuation of impulse response in underwater environment [19], which provides an estimation of the channel gain within the link range. When the diffusion length is below 15 and the data rates are lower than 50 Mbps [11], [19], it can be estimated by (3). Under these conditions, the channel can be treated as non-dispersive, and the inter-symbol-interference (ISI) is negligible.

$$h(d) = a_1 e^{-c_1 d} + a_2 e^{-c_2 d}, \tag{3}$$

where the variable d is the underwater communication distance, the received optical power varies significantly with the communication distance, and is also influenced by different bias current conditions. Indeed, the transmitted luminous flux F_I is a quadratic function of the forward bias current I_b [20],

$$F_I = aI_b^2 + bI_b + c, \tag{4}$$

where a, b, and c are constant parameters. As a result, the received luminous flux could be obtained by

$$\psi = F_I h(d) + F_b, \tag{5}$$

where F_b is the background luminous flux, and the values of a_1, c_1, a_2, and c_2 refer to the parameters in the clean ocean with a half power angle of 10° [21].

B. GFC Method for Mobile Communication

The key point of GFC in underwater wireless optical communication is to implement a dynamic detection mechanism for fluctuating signals caused by variations in optical power, with a wide dynamic range. This mechanism is characterized by fast tracking and low fluctuation.

We setup a feedback mechanism by establishing a linear relationship between the gain control parameter and the threshold, that is

$$G_g = T_r k + f, \tag{6}$$

where k and f are constants, and a dynamic threshold is obtained for discerning between high and low levels within a bit interval.

As depicted in Fig. 1, the cumulative average of amplitudes classified as high level and low level are calculated respectively for each fixed-length continuous sampled amplitude, and counting the number of amplitudes of both levels, respectively. The dynamic threshold T_{r} represents the average of the sampled amplitudes corresponding to intervals of both levels. In Addition, the first data frame is employed as a training sequence to initialize the threshold, which undergoes dynamic updates in response to variations in the sampled data. A head is embedded within the data frame for data synchronization purposes.

In order to evaluate the impact of transceiver mobility on performance, different threshold mechanisms were employed in

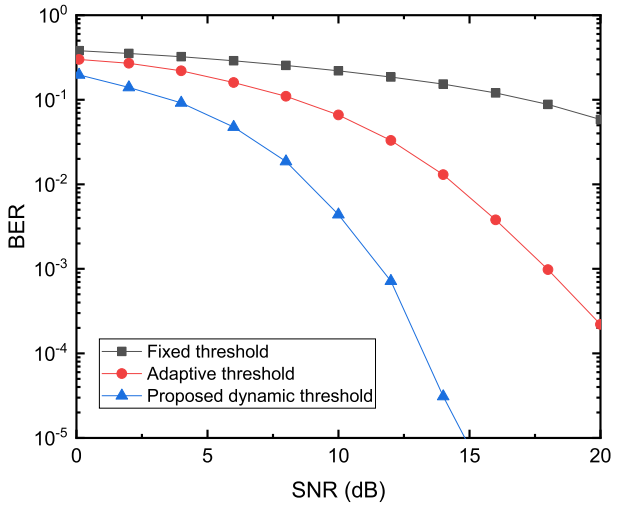

Fig. 2. Performance in simulation under different threshold mechanism.

the simulation of real-time demodulation. A sequence of random amplitude variation was introduced during data transmission to simulate the scenario where the amplitude of the signal fluctuates due to movement. During the data transmission, the received signal was continuously sampled by the analog-to-digital converter (ADC), and the update of dynamic threshold played a key role in real-time demodulation under different SNR conditions. The simulation results are shown in Fig. 2.

As shown in Fig. 2, it is evident that the system with a fixed threshold proved ineffective in different SNR situations, when the amplitude of the received signals significantly fluctuates. The system with an adaptive threshold systems exhibits improved fault tolerance compared with fixed threshold systems, however, their inferior performance to dynamic mean threshold systems due to the application of binary hard decision-making. As a result, by establishing appropriate thresholds at the receiver, the accuracy of signal recognition can be improved in cases of rapidly changing signals caused by unstable channel conditions.

To evaluate the dynamic range of the system with GFC, we also simulated the dynamic range of communication distance and minimum distance for different I_b values using the parameters listed in Table I, which coincide with our experimental conditions. The calculated result is shown in Fig. 3. It can be observed that as the forward bias current I_b value increases, both the minimum communication distance and dynamic range of communication distance continue to increase. Moreover, the minimum communication distance with GFC is smaller in comparison with that without GFC, while the dynamic range with GFC is greater than that without GFC, showing an increase by a factor of more than 7.1. Consequently, the adopted method with GFC can effectively improve the dynamic range of communication distance.

III. Experiment Result

The transceiver used for underwater visible light mobile communication experiments is depicted in Fig. 4. Reflective

TABLE I
Simulation Parameters

Parameter	Value
a_1	0.05
c_1	0.16
a_2	0.12
c_2	0.51
a	-102
b	309
c	3.65
m	61.02
n	4.7×10^7
g_m	10000
k	-1.25
f	1.5
V_{out} (V)	[0.8,1.6]
S (m^2)	0.0007
F_b (lm)	0.02

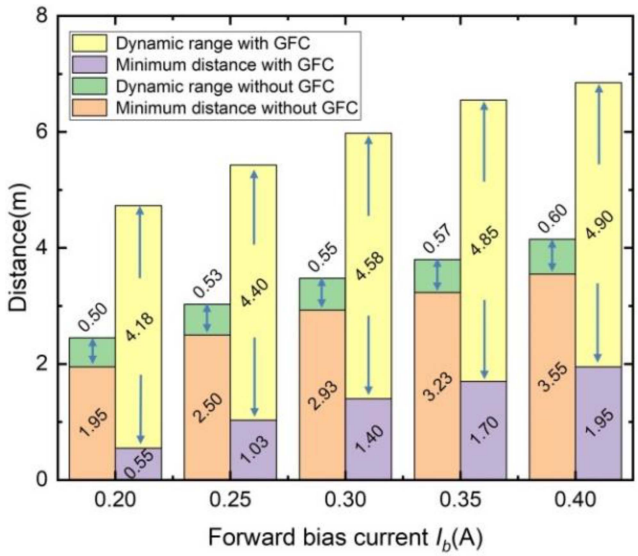

Fig. 3. Dynamic range of communication distance and minimum distance as a function of forward bias currents with and without GFC.

cups are employed at both the transmitter and receiver sides for collimation purposes. Since the intrinsic absorption of water is minimized at blue light wavelength region, a commercially available LED (Cree XPE-2-R4), operating at a wavelength of 465 nm, and a compatible photoelectric detector (Hamamatsu S10784) are selected and fixed at the focal points of the reflective cups, respectively. In experiments, the data transmission rate was about 5.0 Mb/s due to the intrinsic bandwidth limitations of the commercially available LED. The experimental setup for underwater visible light mobile communication is shown in Fig. 5.

Two transceivers are fixed onto two watertight boxes, respectively. The watertight boxes are attached to trolleys which

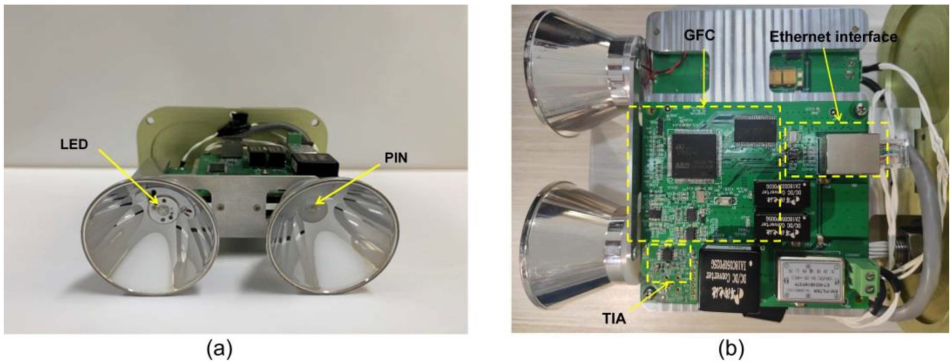

Fig. 4. (a) Side view and (b) top view of transceiver used for experiments.

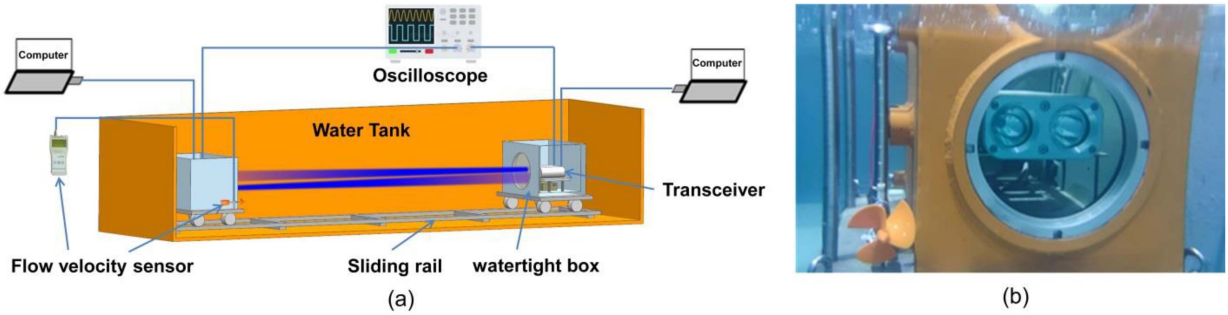

Fig. 5. Schematic of the proposed UVLC system with mobility of transceivers. (a) Experimental setup and (b) photograph of the transceiver inside a watertight box with an installed flow velocity sensor.

Fig. 6. Underwater experiment. (a) Dynamic range of communication distance measurement. (b) Demonstration of real-time video transmission.

could slide along the rails at the bottom of a water tank with a dimension of 1 m $\times$ 0.8 m $\times$ 8 m. The transmitted optical power is measured using an optical power meter (DHC GCI-08), the received signal is detected by a digital storage oscilloscope (KEYSIGHT DSA90804A) with 8 GHz bandwidth, and the moving speed is measured by a flow velocity sensor (NAIWCH LS1206B) with a minimum measurable speed of 0.06 m/s.

In order to verify the performance of UVLC with GFC under mobility of transceivers, the dynamic ranges of communication distance corresponding to the two forward bias currents of 0.30 A and 0.35 A were measured, respectively. Real-time duplex video transmission was also demonstrated as shown in Fig. 6.

First, the duplex links between the transceivers and computers are established, and then we keep one watertight box in stationary and slide the other one on the rails at a speed of 0.21 m/s. The dynamic range of communication distance is obtained when the frames per second (FPS) of the video become zero. In our experiment, the dynamic range of communication distance was measured at forward bias currents of 0.30 A and 0.35 A, respectively. The measured results are shown in Table II.

The relationship between the received signal and the received optical power under different distances was also studied. As depicted in Fig. 7(a), the system with GFC achieves continuous tracking of the output signal and promptly updates the threshold values. Eye diagrams of the output voltage waveform in the

TABLE II
RESULT OF THE DYNAMIC RANGE OF COMMUNICATION DISTANCE MEASUREMENT

Transmitter forward bias current I_b (A)	Video pixels	Communication data rate (Mb/s)	Minimum communication distance (m)	Maximum communication distance (m)	Moving speed of transceiver (m/s)
0.30	800×600	5.0	0.9	5.2	0.21
0.35	800×600	5.0	1.3	5.6	0.21

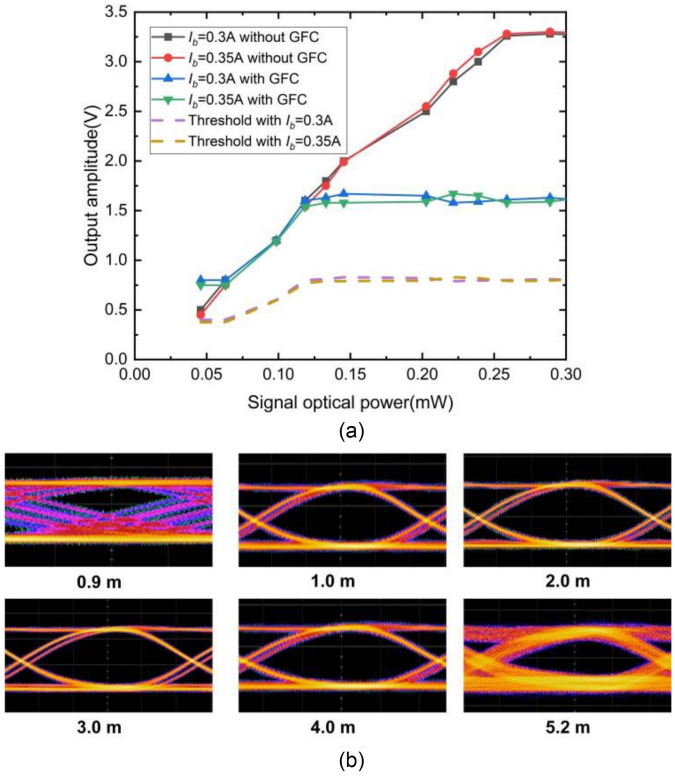

Fig. 7. Transmission experiments. (a) Signal output amplitude versus optical power with and without GFC under different forward bias I_b currents values. (b) Measured eye diagrams with GFC when I_b is 0.30 A under different communication distances.

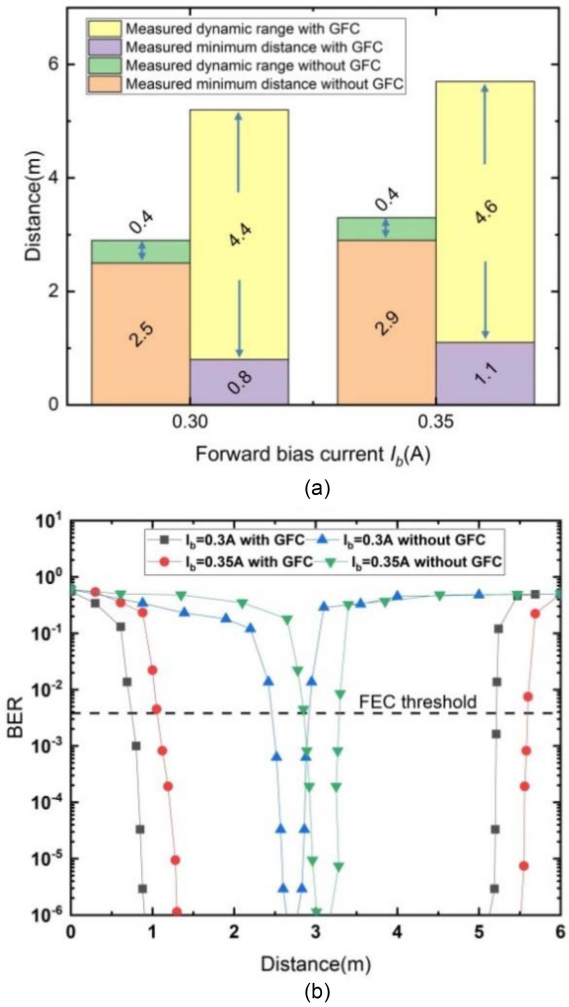

Fig. 8. (a) Measured dynamic range of communication distance with a data rate of 5.0 Mb/s and (b) measured BER curves.

receiver are measured as shown in Fig. 7(b) with a transmitter's forward bias current of 0.30 A. The eye diagrams degrade when the incident optical power is either too weak or too strong due to the influence of system noise and the amplifier's gain limitation respectively. The GFC method demonstrates the ability to achieve dynamic detection and expand the dynamic range while maintaining signal quality without significant degradation. However, the decline in signal quality is caused by the excessive optical power at minimum range, which exceeds the gain limitations of the TIA.

The measured dynamic range of communication distance and the measured bit error rate (BER) as a function of it under different forward bias currents are shown in Fig. 8(a) and (b), respectively. Under a BER threshold of 3.8×10^{-3} assuming 7% forward error correction (FEC) overhead, the dynamic range of communication distance of the system with GFC is improved by a factor of 10.0 and 10.5 in comparison with the system without GFC, respectively, which is slightly better than the theoretical predictions. It implies that the system with GFC is more robust in actual underwater mobile communication scenarios during the movement of the transceiver.

The dynamic range of the receiving FOV angle was also measured both with and without GFC, at a distance of 2.7 m under a bias current of 0.30 A and a distance of 3.0 m under a bias current of 0.35 A, respectively. In our experiment, the receiver was horizontally rotated on a platform inside a watertight box. Fig. 9(a) depicts the measured BER as a function of the receiving FOV angle, while Fig. 9(b) illustrates the measured receiving

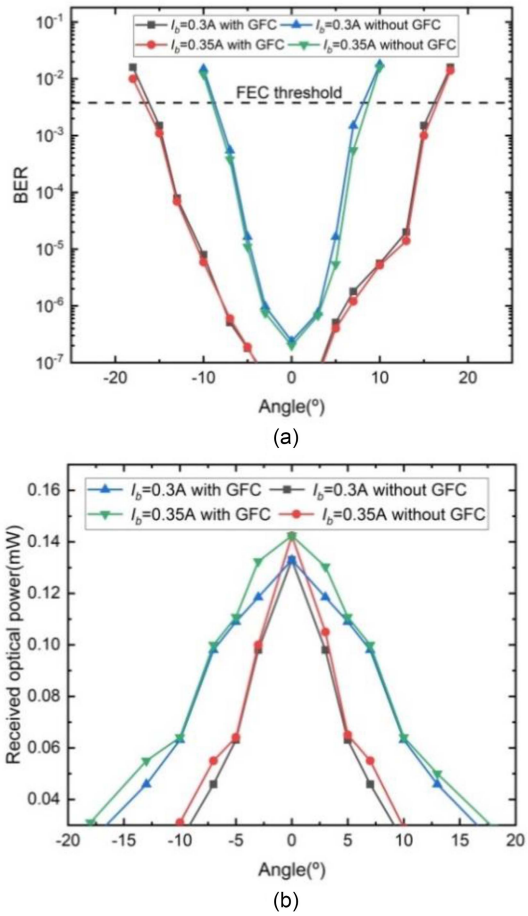

Fig. 9. (a) Measured BER curves at different receiving FOV angles and (b) measured receiving optical power curves at different receiving FOV angles.

optical power as a function of the receiving FOV angle. It can be observed in Fig. 9 that the receiving FOV angle of the system with GFC can be increased by a factor of 1.9 in comparison with the system without GFC. The increase in the receiving FOV angle is helpful for improving the tolerance of positioning in the UVLC system with mobility of transceivers.

IV. Conclusion

In this paper, we propose an UVLC system with mobility of transceivers using a GFC method with dynamic threshold, which obtains significant improvements in both the dynamic range of communication distance and FOV. In experiments, we achieved duplex mobile video transmission with a data rate of 5.0 Mb/s at a moving speed of 0.21 m/s. Real-time duplex video transmission with a resolution of 800 $\times$ 600 pixels was realized at a distance ranging from 1.3 m to 5.6 m. Under a BER threshold of 3.8×10^{-3}, the dynamic range of communication distance is increased by a factor of 10.0 and 10.5 in comparison with the system without GFC at forward bias currents of 0.3 A and 0.35 A, respectively. In addition, the receiving FOV angle of the system is increased by a factor of 1.9. A low-cost, high-integrated system and GFC method with dynamic threshold can effectively improve the stability and reliability of UVLC with mobility of transceivers, which may have good potential in underwater mobile communication applications.

Reference

[1] P. Zou, Y. Zhao, and F. Hu, "Underwater visible light communication at 3.24 Gb/s using novel two-dimensional bit allocation," *Opt. Exp.*, vol. 28, no. 8, pp. 11319–11338, 2020.

[2] F. Wang, Y. Liu, and M. Shi, "3.075 Gb/s underwater visible light communication utilizing hardware pre-equalizer with multiple feature points," *Opt. Eng.*, vol. 58, no. 5, 2019, Art. no. 056117.

[3] M. Chen, P. Zou, L. Zhang, and N. Chi, "Demonstration of a 2.34 Gbit/s real-time single silicon-substrate blue LED-based underwater VLC system," *IEEE Photon. J.*, vol. 12, no. 1, Feb. 2020, Art. no. 7900211.

[4] R. Bian, I. Tavakkolnia, and H. Haas, "15.73 Gb/s visible light communication with off-the-shelf LEDs," *J. Lightw. Technol.*, vol. 37, no. 10, pp. 2418–2424, May 2019.

[5] T. Sawa, JAMSTEC, "Study of adaptive underwater optical wireless communication with photomultiplier tube," Jul. 26, 2017. [Online]. Available: https://www.godac.jamstec.go.jp/cr_catalog/external/metadata/KR17-11_leg2_all/file/KR17-11_leg2_all.pdf

[6] S. Fasham and S. Dunn, Sonardyne, "Bluecomm 200 – optical communications system," Sep., 2023. [Online]. Available: https://www.sonardyne.com/wp-content/uploads/2021/07/Sonardyne_8361_BlueComm_200.pdf

[7] Y. Mu, C. Wang, X.-X. Du, and Y. J. Zhu, "Optimal bias current design for visible light communications based on LED electrical-thermal effect," *IEEE Photon. J.*, vol. 25, no. 6, Dec. 2021, Art. no. 7300706.

[8] X. Li et al., "Wireless visible light communications employing feed-forward pre-equalization and PAM-4 modulation," *J. Lightw. Technol.*, vol. 34, no. 8, pp. 2049–2055, Apr. 2016.

[9] H. M. Oubei et al., "Simple statistical channel model for weak temperature-induced turbulence in underwater wireless optical communication systems," *Opt. Lett.*, vol. 42, no. 13, pp. 2455–2458, 2017.

[10] E. Zedini, H. M. Oubei, A. Kammoun, M. Hamdi, B. S. Ooi, and M.-S. Alouini, "Unified statistical channel model for turbulence-induced fading in underwater wireless optical communication systems," *IEEE Trans. Commun.*, vol. 67, no. 4, pp. 2893–2907, Apr. 2019.

[11] S. Tang, Y. Dong, and X. Zhang, "Impulse response modeling for underwater wireless optical communication links," *IEEE Trans. Commun.*, vol. 62, no. 1, pp. 226–234, Jan. 2014.

[12] M. V. Jamali et al., "Statistical distribution of intensity fluctuations for underwater wireless optical channels in the presence of air bubbles," in *Proc. Iran Workshop Commun. Inf. Theory*, 2016, pp. 1–6.

[13] Z.-Y. Wu, M. Ismail, J. Kong, E. Serpedin, and J. Wang, "Channel characterization and realization of mobile optical wireless communications," *IEEE Trans. Commun.*, vol. 68, no. 10, pp. 6426–6439, Oct. 2020.

[14] K. R. Sekhar, F. Miramirkhani, R. Mitra, and A. C. Turlapaty, "Generic BER analysis of VLC channels impaired by 3D user-mobility and imperfect CSI," *IEEE Commun. Lett.*, vol. 25, no. 7, pp. 2319–2323, Jul. 2021.

[15] J.-S. Xue, Y.-Y. Zhang, and Y.-J. Zhu, "Integrated frame coding for short burst transmission in mobile visible light communication systems," *IEEE Photon. J.*, vol. 14, no. 1, Feb. 2022, Art. no. 7312707.

[16] J. Ning, G. Gao, J. Zhang, H. Peng, and Y. Guo, "Adaptive receiver control for reliable high-speed underwater wireless optical communication with photomultiplier tube receiver," *IEEE Photon. J.*, vol. 13, no. 4, Aug. 2021, Art. no. 7300107.

[17] Y. Guo et al., "Compact scintillating-fiber/450-nm-laser transceiver for full-duplex underwater wireless optical communication system under turbulence," *Opt. Exp.*, vol. 30, no. 1, pp. 53–69, 2022.

[18] J. Jin et al., "Adaptive feedback threshold based demodulation for mobile visible light communication and positioning integrated system," *Opt. Exp.*, vol. 30, no. 8, pp. 13331–13344, 2022.

[19] F. Akhoundi, J. A. Salehi, and A. Tashakori, "Cellular underwater wireless optical CDMA network: Performance analysis and implementation concepts," *IEEE Trans. Commun.*, vol. 63, no. 3, pp. 882–891, Mar. 2015.

[20] X. Deng, Y. Wu, A. M. Khalid, X. Long, P. J. Linnartz, and M. G. Linnartz, "LED power consumption in joint illumination and communication system," *Opt. Exp.*, vol. 25, no. 16, pp. 18990–19003, 2017.

[21] C. Wang, H.-Y. Yu, and Y.-J. Zhu, "A long distance underwater visible light communication system with single photon avalanche diode," *IEEE Photon. J.*, vol. 8, no. 5, Oct. 2016, Art. no. 7906311.